IEEE Photonics Journal
An IEEE Photonics Society Publication

Open Access

Optical Fiber Humidity Sensor Based on Water Absorption Peak Near 2-μm Waveband

Volume 11, Number 2, April 2019

Ke Xu, *Member, IEEE*
Haoying Li
Yingjie Liu
Yujie Wang
Jiajun Tian
Liang Wang, *Member, IEEE*
Jiangbing Du, *Member, IEEE*
Zuyuan He, *Senior Member, IEEE*
Qinghai Song

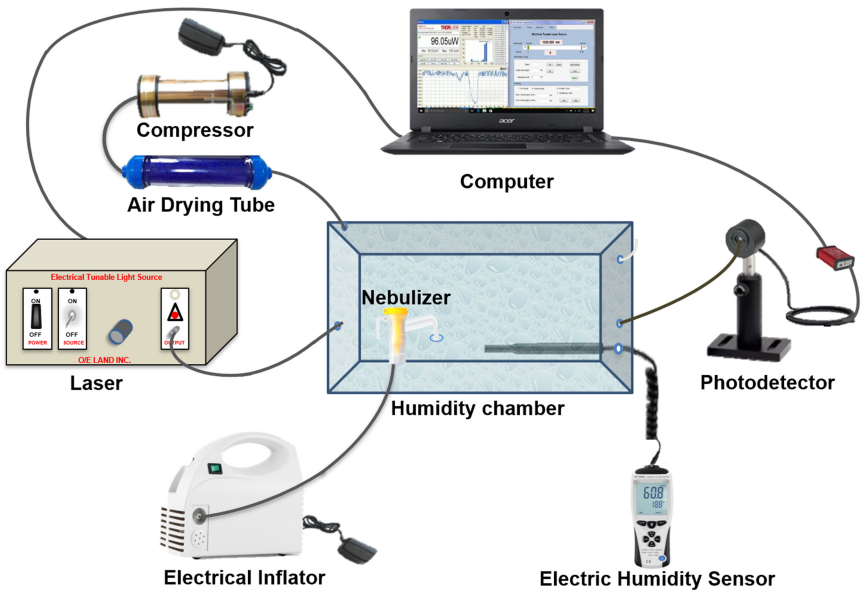

DOI: 10.1109/JPHOT.2019.2901290
1943-0655

Optical Fiber Humidity Sensor Based on Water Absorption Peak Near 2-μm Waveband

Ke Xu,[1] ***Member, IEEE***, **Haoying Li**,[1] **Yingjie Liu**,[1] **Yujie Wang**,[1] **Jiajun Tian**,[1] **Liang Wang**,[2] ***Member, IEEE***, **Jiangbing Du**,[3] ***Member, IEEE***, **Zuyuan He**,[3] ***Senior Member, IEEE***, **and Qinghai Song**[1]

[1]Department of Electronic and Information Engineering, Harbin Institute of Technology, Shenzhen 518055, China
[2]Department of Electronic Engineering, The Chinese University of Hong Kong, Hong Kong
[3]State Key Laboratory of Advanced Optical Communication Systems and Networks, Shanghai Jiao Tong University, Shanghai 200240, China

DOI:10.1109/JPHOT.2019.2901290

Manuscript received January 14, 2019; revised February 15, 2019; accepted February 19, 2019. Date of publication February 25, 2019; date of current version March 13, 2019. This work was supported in part by the National Natural Science Foundation of China under Grants 61875049, 61505039, 61575051, and 61675055, and in part by the Shenzhen Fundamental Research Projects under Grants JCYJ20170307151047646 and JCYJ20170815140136635. Corresponding author: Ke Xu and Liang Wang (email: kxu@hit.edu.cn; lwang@ee.cuhk.edu.hk).

Abstract: We demonstrate the absorption-based fiber humidity sensors working near 1950 nm wavelength which is a strong water absorption peak. No additional coating of humidity-sensitive material is needed for the proposed relative humidity (RH) fiber sensors. Two sensor structures including a taper fiber and a microfiber knot resonator are fabricated. For the taper fiber sensor, upto 0.18 mW/% RH sensitivity has been achieved via direct power measurement. For the fiber knot sensor, the RH variations induce both extinction ratio change and wavelength shift. The optical spectra of the fiber knot resonator under different RH are measured, and the extinction ratio and wavelength shift sensitivity are measured to be 0.034 dB/% RH and 10 pm/% RH, respectively. The response time for the tapered fiber is 1.13 s for RH increasing from 28.6% to 53.4% and 2.27 s for the reverse operation. The microfiber knot sensor can respond in 0.8 and 1.55 s accordingly. The sensor performance for the two structures is also investigated under different temperatures from 25 °C to 45 °C and the results indicate negligible impact from the temperature variations. We believe the simple fabrication and low cost of the sensor will make it potential and practical for the RH measurement.

Index Terms: Fiber optics sensors, 2-μm spectral range.

1. Introduction

The relative humidity (RH) of the air is an important parameter in various scenarios such as agricultural environment, ecological application, material storage, automated control process, meteorology, biomedical measurement and so forth [1]. While conventional RH measurement has been reported via a wide scope of techniques based on mechanical and electronic approaches, optical fiber-based techniques have shown greater potential for RH sensing [2]. Fiber optic RH sensors offer distinct advantages like remote monitoring, light weight, compact size, easy multiplexing,

immunity to electromagnetic disturbance, etc. Due to the mature and widely available components at C-band wavelengths, a plenty of demonstrations of fiber optic RH sensors working at 1.5 μm wavelength range have been reported. Most commonly demonstrated schemes mainly include the use of fiber Bragg gratings [3]–[5], fiber interferometers [6]–[9], resonant cavities [10]–[12], fiber evanescent waves [13]–[15], etc. The operation mechanisms for these techniques are either based on refractive index change induced by the moisture in contact with the fiber or the absorption by the humidity-sensitive material coated on the fiber surface. The absorption-based technique is always a straightforward way of measuring the humidity, but it has to rely on other materials such as agarose gel, polyimide as the optical wave at C-band is transparent to moisture. Zhang *et al.* reported a diameter tapered multimode-fiber-based humidity sensor with Gelatin material. The sensor can measure the RH ranges from 9%-94% with less than 0.5s response time [16]. Fuke *et al.* demonstrated an absorbance measurement of a U-bend multimode fiber sensor covered by Ag-Polyaniline. The sensor can operate from 5% RH to 95% RH but the response time is 30s [17]. More recently, Li *et al.* demonstrated a power loss measurement of a fiber coated with PVA which can sense the RH from 30%-90%, but the sensitivity is only 1.994 μW/% RH [18].

Recently, 2-μm waveband emerged as a potential new spectral resource for optical communications [19]–[22]. Significant amount of attention has been attracted to the optical components operating at 2-μm wavelengths [23]–[26]. Narrow line width laser, optical amplifier, high-speed photo detector, and low-loss single mode fiber have been reported very recently. Apart from the potential for carrying information using the optical wave at 2-μm band, the other distinct feature of this spectral window is the coverage of a strong water absorption band near 1950 nm [27], [28]. It can potentially enable an all-fiber and absorption type RH sensor. In this paper, we demonstrate such an all-fiber RH sensor without coating of any moisture sensitive materials which results in an easier fabrication process and potential lower cost. The proposed fiber sensor is based on the strong water absorption of the fiber evanescent wave near 1950 nm wavelength. Such absorption-based fiber sensor is easy to operate and implement. Besides, it allows for remote sensing and can be easily multiplexed to parallel channels. To demonstrate the possible RH sensing application at 2-μm waveband, we fabricate two types of microfiber devices: tapered fiber and a fiber micro-knot. Both structures allow for strong evanescent wave generation and easy exposure of the optical wave in air for absorption by the moisture in air. We have characterized the proposed fiber sensors in a sealed and RH-variable environment. The sensitivity, time response, and stability of both device structures for RH measurement are analyzed and discussed.

2. Sensor Fabrication and Experimental Setup for RH Measurement

To generate the evanescent wave, we first fabricate a tapered microfiber. We fabricate the tapered fiber by clamping a single-mode fiber on a pair of stepper motor translation stages. The central part of the fiber is suspended and is heated by hydrogen-oxygen flame. The fiber waist can be gradually thinned by the reverse traction force of the stepping motor. In the meantime, the flame scanning is repeatedly performed to ensure the uniformly reduction of the taper waist diameter. More details for the fabrication of tapered fiber can be found elsewhere. Here, we fabricate a tapered fiber with the minimum diameter of the tapered waist is about 1 μm and the microscope image is shown in Fig. 1(a).

On the other hand, we also fabricate another type of fiber device which is the microfiber knot resonator (MKR) for better enhancement of the evanescent wave absorption. It consists of a tapered fiber knot with very small bending radius. Such structure allows for optical field enhancement within the cavity and exposes a significant amount of optical wave in the air. First of all, a stable and clean environment is required for such device preparation process. To prepare a MKR, one end of the single mode fiber is fixed on the two-dimensional translation stage and the other end is pulled to the opposite direction by an alcohol-sterilized tweezer. At the same time, the flame gradually heats up and melts the fiber cladding. Then, a probe is used to tie the tapered region into a knot. The success of this process requires the precise control of the speed of fiber stretching and the

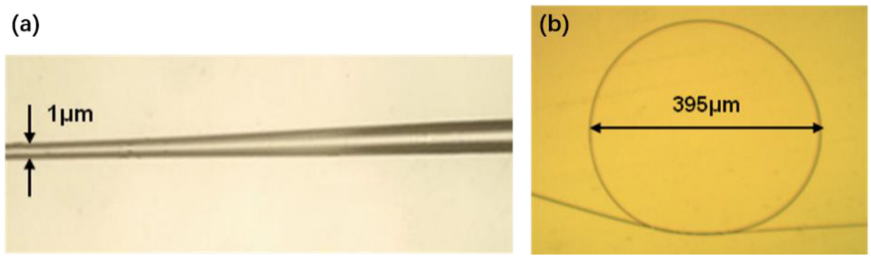

Fig. 1. (a) The sensing region of the tapered fiber under the optical microscope. (b) The microscope image of the micro fiber knot resonator.

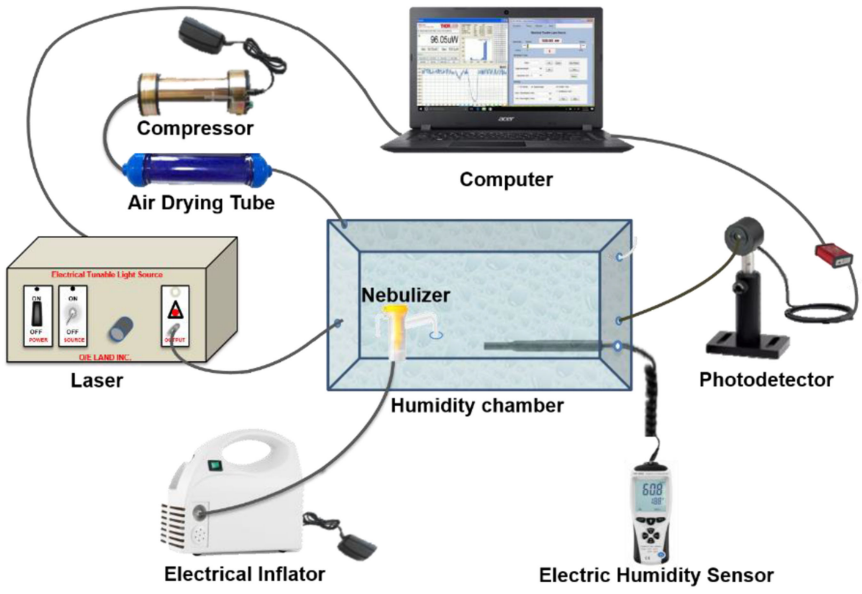

Fig. 2. The experimental setup for the RH measurements.

flame movement. The microscope image of the fabricated MKR is shown in Fig. 1(b) and the knot diameter is measured to be $\sim$395 μm.

The experimental setup for the RH measurement is shown in Fig. 2. The optical source is a tunable laser (OETLS-300) which can operate from 1950 nm to 2050 nm with 0.01 nm wavelength step resolution. It should be noted that a more compact laser diode with fixed wavelength near the water absorption peak is also available and can reduce the system cost. The laser output is sent to either the tapered microfiber or the MKR which is placed in a sealed chamber with a dimension of 30 cm $\times$ 15 cm $\times$ 10 cm and RH tunability from 28% to 98%. A commercial electric humidity sensor is used as a reference to monitor the real-time humidity in the chamber. The output from the fiber sensor is coupled out from the chamber and fed into an InGaAs photodetector which has a wavelength response from 1200 nm to 2500 nm (THORLABS, S148C). The laptop computer is used to control the laser and the photo detector. As shown in Fig. 2, the RH inside the chamber is dynamically controlled in this way: the RH can be increased by injection of moisture into the chamber via a nebulizer and an electrical inflator. On the other hand, the RH can be decreased by pumping the moisture out of the chamber via a compressor and an air-drying tube. The fiber sensor is mounted inside the chamber, and its output optical power or spectrum will vary according to the RH change inside the chamber. Finally, the results can be obtained and analyzed in the computer.

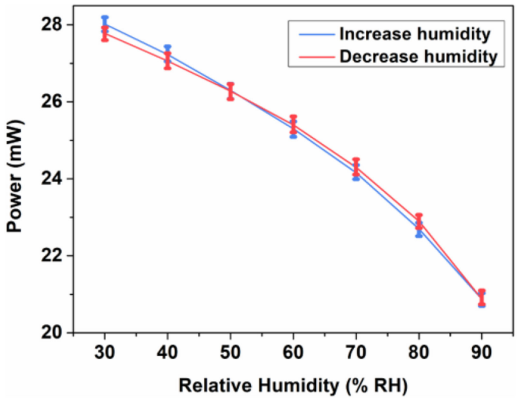

Fig. 3. The measured output optical power of the taper fiber sensor as a function of the RH under repeated humidification and dehumidification process.

3. Results and Discussions

3.1 Tapered-Fiber-Based Humidity Sensor

We loaded the tapered fiber sensor into the chamber and mounted it on the stage. Prior to the RH measurement, the moisture was pumped out first to set a dry condition for the chamber. After a short period of time, the RH drops and stabilized at ∼28% which is the minimum level of RH that we can achieve for the current apparatus. Throughout the whole process, the RH inside the chamber is assumed to be isotropic and is monitored by an electrical RH sensor for reference. The optical power (continuous wave at 1960 nm) launched into the fiber sensor is 18.5 dBm and we measure the output power received by the photodetector. Then, the humidity chamber is gradually humidified by inflating the moisture into the chamber. As the RH increases gradually from 28% to 90% (reading from the RH monitor), the received optical power at the output drops accordingly. We recorded the output power for every 10% increase in RH and plotted the results in Fig. 3. The optical power steadily drops from 28.02 mW to 20.88 mW during this humidifying process. To avoid the interference of temperature on the experimental results, the temperature of the humidity chamber is kept constant at 25 °C ± 0.1 °C. To investigate the bi-directional response of the fiber sensor, we pumped out the moisture from the chamber. In the meantime, we recorded the optical power for every 10% decrease in RH. The results for the drying process are shown as red curve in Fig. 3 and it is quite consistent with the humidifying process. This indicates good repeatability for the humidity sensing based on the eater absorption of the evanescent wave in the tapered fiber at 2-μm waveband. The sensitivity of the proposed tapered fiber humidity sensor is calculated to be ∼0.11 mW/% RH in the low RH region and 0.18 mW/% RH in the high RH regime. The error bar in Fig. 3 is plotted to show the power fluctuation during the power recording. For a moderate RH of 50% and temperature of 25 °C, we have shown the results of 30 consecutive measurements in Fig. 4(a). It reveals that the experimental error is ∼ 0.33 mW. To further investigate the stability of the RH sensing by the tapered fiber, we fix the laser output and stabilize the chamber condition to RH of 30% and 90%, respectively. We record the optical power every 30 min and plot the results in Fig. 4(b). It can be seen that the output optical power only fluctuates within a very limited range for 3 hours. An obvious power contrast between two RHs is also observed which is due to the water absorption at this wavelength.

We also characterize the temporal response of our tapered-fiber-based RH sensor. In this process, we first stabilize the humidity chamber with a RH around 28.6% and a fluctuation of ±0.2%. Then, we open the lid of the humidity chamber and expose it to the air outside. As a result, the RH in the chamber is quickly increased to 53.4%. By closing the lid and increasing the moisture gas flow quickly, then the RH drops to 28.9% rapidly. By doing so, we can switch the RH level inside the chamber within a very short period. During this process, the temperature is carefully maintained

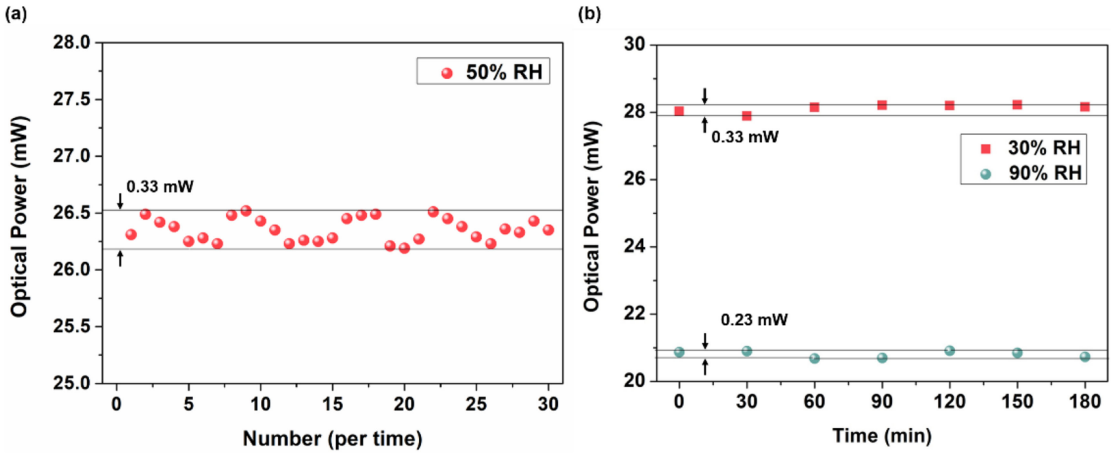

Fig. 4. (a) The output power evolution for 30 consecutive measurements. (b) The output optical power of the tapered fiber sensor as a function of time within 3 hours at 30% RH and 90% RH, respectively.

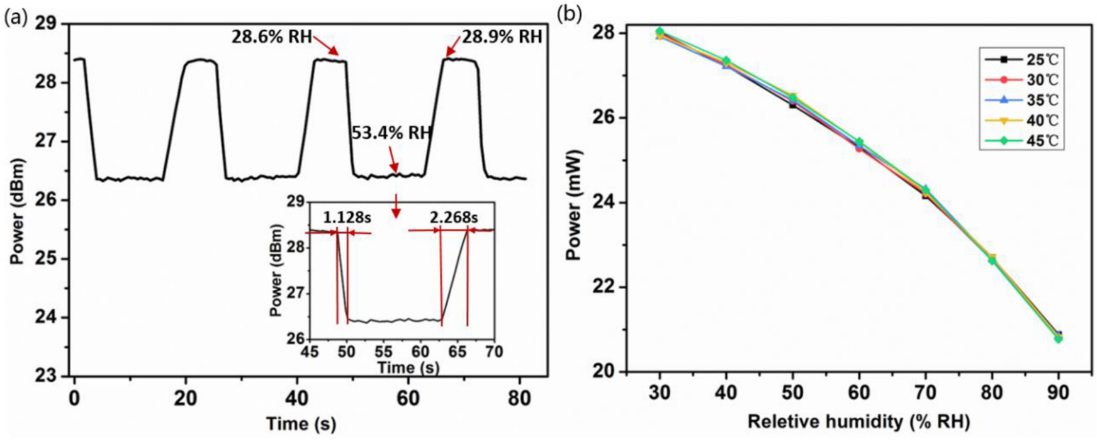

Fig. 5. (a) Temporal response of the tapered fiber sensor when the humidity is rapidly changed from 28.6% RH to 53.4% RH. (b) The output power of the tapered fiber sensor as a function of RH under different temperatures.

at 25 °C ± 0.1 °C. Fig. 5(a) shows the temporal response of the tapered fiber sensor when the humidity is rapidly changing between two different RH levels. The measured rising time for RH increasing from 28.6% to 53.4% is 1.128s and the falling time for RH decreasing from 53.4% to 28.9% is 2.268s. For continuous switching between the two RH levels, the optical power can quickly respond to the switching within a short period of one or two seconds. It should be noted that the temperature variation is one of the critical issues for many refractive-index-based fiber sensors. Here we measure the humidity sensing curve under different temperatures. The curves are plotted in Fig. 5(b) which shows the sensor response for a temperature range from 25 °C to 45 °C. The results show that the impact of the temperature variation on the sensor performance is negligible with a maximum power fluctuation of 0.23 mW.

3.2 Microfiber-Knot-Resonator-Based Humidity Sensor

We also investigate the RH sensing based on the water absorption of the evanescent wave in MKR at 2-μm waveband. The MKR was fabricated and loaded into the humidity chamber. The humidifying

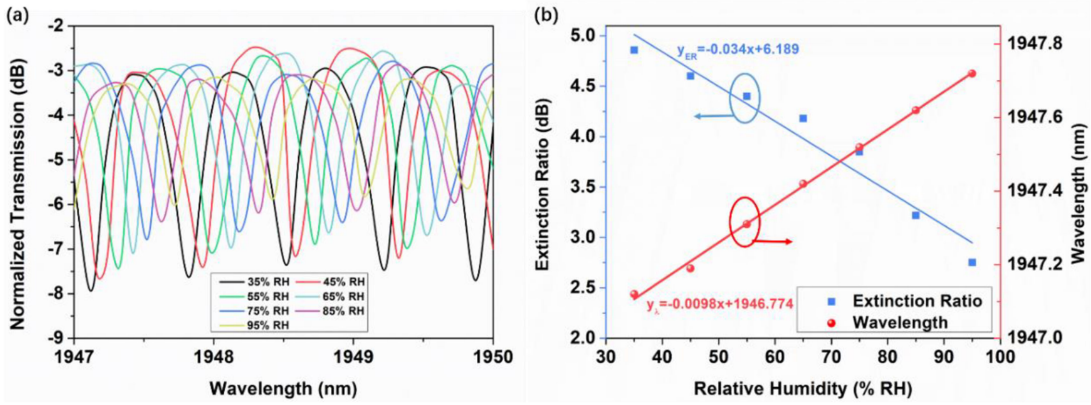

Fig. 6. (a) The normalized transmission spectra of the MKR sensor under different RH. (b) The extinction ratio and the resonant wavelength as a function of RH.

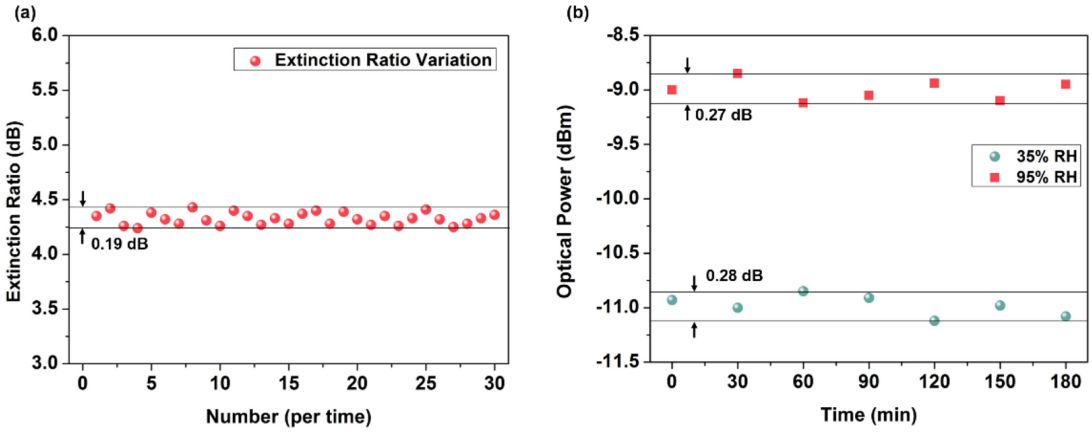

Fig. 7. (a) The extinction ratio variation for 30 consecutive measurements at resonance near 1947.1 nm under RH of 57%. (b) The output optical power variation of the MKR sensor within 3 hours at 35% RH and 95% RH, respectively.

or drying process is similar to the aforementioned procedure, and we measure the transmission spectrum of the MKR under different RH. We scanned the laser wavelength from 1947 nm to 1950 nm and measured the optical power at the output of the MKR sensor. The transmission spectra of the sensor under RH from 35% to 95% are shown in Fig. 6(a). The spectral resonance of the MKR is shifted and the extinction ratio of the spectral resonance is changed when the RH is varied. The resonance shift is caused by the refractive index increase when the water molecules accumulate around the fiber. The extinction ratio reduction at high RH is due to the absorption of light inside the cavity. As shown in Fig. 6(b), we plot the extinction ratio and the resonance wavelength as a function of RH which can be fitted by a linear function. Thus, both resonance wavelength shift and the extinction ratio can be used to monitor the RH. The slope of the linear fitting curve indicates the sensitivity of the MKR humidity sensor, i.e., 0.034 dB/% RH for extinction ratio and 10 pm/% RH for resonance wavelength shift measurement, respectively.

To investigate the stability of the MKR sensor, we stabilize the RH of the chamber to 57%, 25 °C. Then, we record the optical spectra of the resonance near 1947.1 nm and the corresponding extinction ratios for 30 consecutive measurements. In Fig. 7(a), we show that the extinction ratio for the 30 consecutive measurements fluctuates within 0.19 dB. We also monitor the optical power fluctuation at the resonance peak near 1947.1 nm for every 30 minutes and show the results in

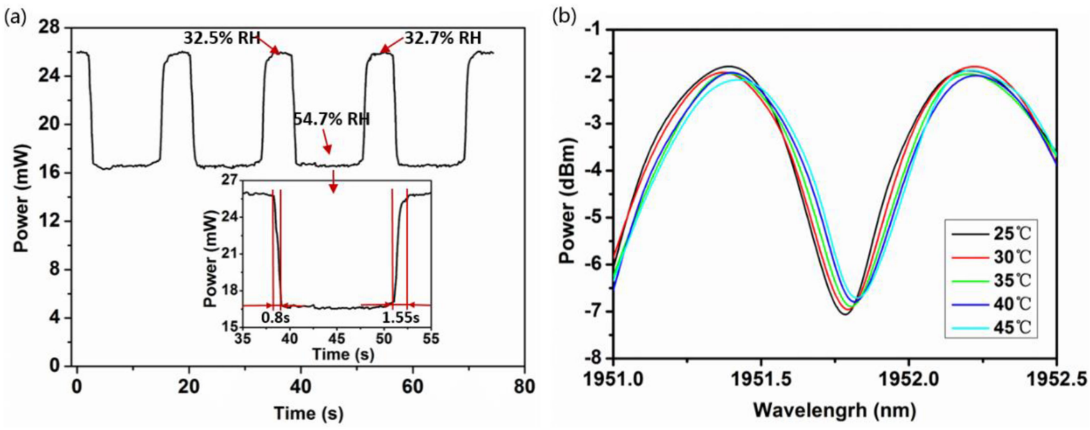

Fig. 8. (a) Temporal response of the MKR sensor when RH is rapidly switched between 32.5% RH and 56% RH. (b) The transmission spectra the MKR sensor at different temperatures when the RH is fixed at 57%.

Fig. 7(b). Under both RH of 35% and 95%, the resonant power fluctuation within 3 hours has a minimum value of 0.28 dB and 0.27 dB respectively which is insignificant. Both fluctuations in extinction ratio and the optical power at resonance peak are due to the fact that it is difficult to perfectly control the RH inside the chamber, which is confirmed by the referenced electric humidity sensor.

Similar measurement is taken to study the temporal response of the MKR sensor. Here, the RH inside the chamber is rapidly switched between 32.6 $\pm$ 0.1% and 54.4% which are calibrated by the electric RH sensor. The laser wavelength is fixed around 1948.1 nm. Under the fast switching between two RH levels, the MKR sensor also responded very fast, as shown in Fig. 8(a). The measured rising time is 0.8s and the falling time is 1.55s which are a bit shorter than those for the tapered fiber sensor. This is due to the longer interaction fiber length between the moisture and the optical wave. Fig. 8(b) shows the transmission spectrum of the MKR sensor under a temperature range from 25 °C to 45 °C with a fixed RH of 57%. It can be seen that the wavelength drift is smaller than 0.1 nm when the temperature increases from 25 °C to 45 °C. The temperature sensitivity for the extinction ratio and wavelength drift are 0.03 dB/ °C and 2.2 pm/ °C, respectively.

4. Conclusion

In summary, we have demonstrated the absorption-based fiber humidity sensor via a microfiber taper and a microfiber knot resonator without coating of additional moisture sensitive material. The two fiber structures enable strong water molecule absorption near 1950 nm when the generated strong evanescent wave interacts with the moisture in the air. The performance of the proposed fiber humidity sensors are characterized and analyzed in terms of sensitivity, temporal response, and stability for RH measurement. Successful static and dynamic RH sensing have been demonstrated with good sensitivity and stability for both structures without significant impact from the temperature variation. Compared with most of the reported fiber humidity sensors, our scheme has the advantages of simple fabrication and low cost, enabled by direct sensing measurement via water molecule absorption peak near 2-μm waveband.

References

[1] N. Yamazoe, “Humidity sensors: Principles and applications,” *Sens. Actuators*, vol. 10, no. 3/4, pp. 379–398, 1986.
[2] L. Alwis, T. Sun, and K. T. V. Grattan, “Optical fibra-based sensor technology for humidity and moisture measurement: review of recent progress,” *Measurement*, vol. 46, 4052–4074, 2013.

[3] G. Woyessa, K. Nielsen, A. Stefani, C. Markos, and O. Bang, "Temperature insensitive hysteresis free highly sensitive polymer optical fiber Bragg grating humidity sensor," *Opt. Exp.*, vol. 24, no. 2, pp. 1206–1213, 2016.
[4] A. Urrutia, J. Goicoechea, A. Ricchiuti, D. Barrera, S. Sales, and F. J. Arregui, "Simultaneous measurement of humidity and temperature based on a partially coated optical fiber long period grating," *Sensors Actuators B Chem.*, vol. 227, pp. 135–141, 2016.
[5] X. F. Chen, W. Zhang, C. Liu, H. Hong, and D. J. Webb, "Enhancing the humidity response time of polymer optical fiber Bragg grating by using laser micromachining," *Opt. Exp.*, vol. 23, no. 20, pp. 25942–25949, 2015.
[6] P. Hu, X. Dong, K. Ni, L. Chen, W. Wong, and C. Chan, "Sensitivity-enhanced michelson interferometric humidity sensor with waist-enlarged fiber bitaper," *Sensors Actuators B Chem.*, vol. 194, pp. 180–184, 2014.
[7] B. Wang, J. Tian, L. Hu, and Y. Yao, "High sensitivity humidity fiber-optic sensor based on all-agar Fabry–Perot interferometer," *Sensors J.*, vol. 19, no. 12, pp. 4879–4885, 2018.
[8] J. Shi *et al.*, "Humidity sensor based on Fabry-Perot interferometer and intracavity sensing of fiber laser," *J. Lightw. Technol.*, vol. 35, no. 21, pp. 4789–4795, Nov. 2017.
[9] J. Mathew, Y. Semenova, and G. Farrell, "Relative humidity sensor based on an agarose-infiltrated photonic crystal fiber interferometer," *J. Sel. Topics Quantum Electron.*, vol. 18, no. 5, pp. 1553–1559, 2012.
[10] P. Wang, F. Gu, L. Zhang, and L. Tong, "Polymer microfiber rings for high-sensitivity optical humidity sensing," *Appl. Opt.*, vol. 50, no. 31, pp. G7–G10, 2011.
[11] J. Lou, Y. Wang, and L. Tong, "Microfiber optical sensors: A review," *Sensors*, vol. 14, no. 4, pp. 5823–5844, 2014.
[12] Y. Wu, T. Zhang, Y. Rao, and Y. Gong, "Miniature interferometric humidity sensors based on silica/polymer microfiber knot resonators," *Sensors Actuators B Chem.*, vol. 155, pp. 258–263, 2011.
[13] Y. Tan, L. Sun, L. Jin, J. Li, and B. Guan, "Temperature-insensitive humidity sensor based on a silica fiber taper interferometer," *Photon. Technol. Lett.*, vol. 25, no. 22, pp. 2201–2204, 2013.
[14] D. Liu *et al.*, "High sensitivity refractive index sensor based on a tapered small core single-mode fiber structure," *Opt. Lett.*, vol. 40, no. 17, pp. 4166–4169, 2015.
[15] Y. Liu, Y. Zhang, H. Lei, J. Song, H. Chen, and B. Li, "Growth of well-arrayed ZnO nanorods on thinned silica fiber and application for humidity sensing," *Opt. Exp.*, vol. 20, no. 17, pp. 19404–19411, 2012.
[16] L. Zhang, F. Gu, J. Lou, X. Yin, and L. Tong, "Fast detection of humidity with a subwavelength-diameter fiber taper coated with gelatin film," *Opt. Exp.*, vol. 16, pp. 13349–13353, 2008.
[17] M. V. Fuke, P. Kanitkar, M. Kulkarni, B. B. Kale, and R. C. Aiyer, "Effect of particle size variation of Ag nanoparticles in polyaniline composite on humidity sensing," *Talanta*, vol. 81, pp. 320–326, 2010.
[18] T. Li, X. Dong, C. C. Chan, C. Zhao, and P. Zu, "Humidity sensor based on a multimode-fiber taper coated with polyvinyl alcohol interacting with a fiber Bragg grating," *IEEE Sensors*, vol. 12, no. 6, pp. 2205–2208, Jun. 2012.
[19] K. Xu, L. Sun, Y. Q. Xie, Q. Song, J. B. Du, and Z. He, "Transmission of IM/DD signals at 2 μm wavelength using PAM and CAP," *IEEE Photon. J.*, vol. 8, no. 5, Oct. 2016.
[20] K. Xu, Q. Wu, Y. Xie, M. Tang, S. Fu, and D. Liu, "High-speed single-wavelength modulation and transmission at 2μm under bandwidth-constrained condition," *Opt. Exp.*, vol. 25, no. 4, pp. 4528–4534, 2017.
[21] Z. Liu *et al.*, "52.6 Gbit/s single-channel directly-modulated optical transmitter for 2-μm spectral region," in *Proc. Opt. Fiber Commun. Conf.*, 2015, Paper Th1E.6.
[22] H. Zhang *et al.*, "100 Gbit/s WDM transmission at 2 μm: transmission studies in both low-cost hollow core photonic bandgap fiber and solid core fiber," *Opt. Exp.*, vol. 23, no. 4, pp. 4946–4951, 2015.
[23] P. Roberts *et al.*, "Ultimate low loss of hollow-core photonic crystal fibres," *Opt. Exp.*, vol. 13, no. 1, pp. 236–244, 2005.
[24] J. Li *et al.*, "2-μm wavelength grating coupler, bent waveguide, and tunable microring on silicon photonic MPW," *Photon. Technol. Lett.*, vol. 30, no. 5, pp. 471–474, 2018.
[25] Y. Dong *et al.*, "Two-micron-wavelength germanium-tin photodiodes with low dark current and gigahertz bandwidth," *Opt. Exp.*, vol. 25, no. 14, pp. 15818–15827, 2017.
[26] M. U. Sadiq *et al.*, "40 Gb/s WDM transmission over 1.15-km HC-PBGF using an InP-based mach-zehnder modulator at 2μm," *J. Lightw. Technol.*, vol. 34, no. 8, pp. 1706–1711, Apr. 2016.
[27] L. Kou, D. Labrie, and P. Chylek, "Refractive indices of water and ice in the 0.65- to 2.5-μm spectral range," *Appl. Opt.*, vol. 32, no. 19, pp. 3531–3540, 1993.
[28] J. Bertie and Z. Lan, "Infrared intensities of liquids XX: The intensity of the OH stretching band of liquid water revisited and the best current values of the optical constants of H_2O(l) at 25 °C between 15000 and 1 cm^{-1}," *Appl. Opt.*, vol. 50, no. 8, pp. 1047–1057, 1996.